Indian Journal of Fibre & Textile Research
Vol. 41, December 2016, pp. 373-379

Properties of PS/TiO_2 electrospun fibres using limonene as a solvent

Maryam Khirandish[1], Sedigheh Borhani[1, a], Shadpour Mallakpour[2] & Mostafa Youssefi[1]

[1]Department of Textile Engineering, [2]Department of Chemistry, Isfahan University of Technology, Isfahan 84156-83111, Iran

Received 26 October 2014; revised received and accepted 1 June 2015

Limonene, a natural solvent, has been used for producing polystyrene (PS) nanocomposite (NC) fibres. Nanocomposite fibres of PS are prepared by electrospinning of a homogeneous solution of titanium dioxide (TiO_2) nanoparticles (NPs) and PS. X-ray diffraction (XRD) pattern of PS nanocomposite fibres confirms the presence of TiO_2 nanoparticles in the samples. FTIR spectra of PS nanocomposite fibres obviously show that there is no chemical linkage or interaction between PS and TiO_2 nanoparticles in the resulting composites fibres. The morphology of PS electrospun fibres and PS/TiO_2 nanocomposite fibres is investigated by SEM and FE-SEM. FE-SEM images of electrospun fibres reveal some aggregation of TiO_2 nanoparticles. The results also show that increasing TiO_2 nanoparticles reduces PS electrospun fibres diameter. Also, the UV protection of PS electrospun fibres is enhanced due to the increase in TiO_2 nanoparticles load. Tensile strength and elasticity modulus first show an increase up to 4 wt% of TiO_2 and then a decrease at higher loading. Differential scanning calorimeter (DSC) thermograms for PS electrospun fibres indicate that the introduction of TiO_2 nanoparticles decreases the glass transition temperature (T_g).

Keywords: Electrospinning, Limonene, Nanofibres, Nanoparticles, Polystyrene

1 Introduction

Nanotechnology has been well developed during the past two decades with a significantly growing number of studies on nanofibres and their applications[1-4]. In particular, the nanofibres and nanomaterials science in textiles have received much attention, showing various applications. Electrospinning as a simple and inexpensive technique is used for producing fibres with a diameter ranging from submicrometers to nanometers. Electrospun fibre mats, due to their high surface area, small pore size distribution and high porosity, are good candidates that can be employed in many applications[4].

Recently, the use of various types of nanoparticles dispersed in polymer solutions have attracted great interest in nanofibres production because they often show dramatic improvement in the properties of electrospun fibres as compared to virgin fibres[5].

Amorphous polystyrene (PS) is a transparent and commonly used plastic. It is a hard and brittle polymer with very high electrical resistance and low dielectric loss[6]. This versatile polymer, which has several advantages such as no pollution and toxicity, is used in various fields[6]. Electrospinning of PS has also attracted great interest because of its varied applications in areas such as ion exchange[7,8], filtration[9], tissue engineering[10], etc. Numerous researchers have investigated the structure and properties of electrospun PS fibres[11-18]. Common organic solvents such as N, N-dimethyformamide (DMF), tetrahydrofuran (THF), N, N-dimethy lacetamide (DMAc), toluene, etc. are well known as PS solvents in electrospinning[19-23]. These solvents are not environment-friendly because of their toxicity and may emit an unpleasant smell or toxic gases. García *et al.*[24] tested several natural solvents as dissolution agents for extruded polystyrene. Noguchi *et al.*[25], by using d-limonene as a green solvent, developed a method to shrink expanded polystyrene (EPS)[25]. Shin *et al.*[26] produced PS nanofibres with EPS solution using d-limonene[26]. They compared electrospun PS fibre from EPS solution dissolved in d-limonene with PS nanofibre produced from dissolving PS in other solvents such as THF, DMAc, and DMF. It was observed that although d-limonene was a good solvent for polystyrene, at low concentrations, the electrospinning jet stability of PS was poor compared to other solvents.

D-Limonene, a monoterpene hydrocarbon, is a natural and biodegradable solvent. It is the principal component of orange or lemon peel oil[26,27]. As a

[a]Corresponding author.
E-mail: sborhani@cc.iut.ac.ir

solvent, DL-limonene can be used to replace toxic, hazardous, and dangerous organic solvents. D-Limonene has various valuable usages including medical and pharmaceutical products, perfumes, flavorings, pesticides, cleaners, heat transfer fluids, and solvents[26,27].

Electrospinning process of PS is mostly achieved using organic solvents. It has some problems such as environmental problem, difficulty of process handling, solvent costs, and presence of the trace of solvent impurities.

Recently, the use of various types of nanoparticles (NPs) dispersed in PS has been extensively studied to enhance the properties of electrospun PS and consequently, extend its application fields[28-32].

Mazinani *et al*[28] investigated the morphology and properties of PS/carbon nanotube (CNT) electrospun fibres. They used styrene–butadiene–styrene type as an interfacial agent to modify the dispersion of CNTs. The results showed that fibres diameter was decreased by increasing CNT concentration. Also, improvement in electrical conductivity and mechanical properties was obtained by the addition of CNT below percolation. Preparation of bead-free PS/Ni electrospun fibre with higher thermal stability was reported by Chen *et al*[29]. Rojas *et al*[30] revealed that by using cellulose nanowhiskers as the reinforcing material in the electrospinng of PS, the elastic modulus of electrospun fibres was increased with nanowhisker content. Also, T_g of electrospun fibres tended to decrease with increasing cellulose nanowhiskers load. Kim *et al*[31] produced PS/gold nanocomposite (NC) fibres[31]. Based on the results, an increase in gold nanoparticles load resulted in an increase in the surface roughness of electrospun PS/gold fibres and subsequently, a decrease in the diameter and T_g of electrospun fibres. Electrospinning of PS containing zinc oxide and titanium dioxide nanoparticles was reported by Kobayashi e*t al*[32]. They found that the morphology of electrospun fibres was changed by the addition of nanoparticles in PS solutions.

In this study, DL-limonene as a green media was used as a solvent for PS. PS/TiO_2 nanocomposite fibres with different TiO_2 nanoparticles loadings were electrospun. The effect of the concentration of TiO_2 nanoparticles on the properties of PS electrospun fibres was investigated. The morphology of the electrospun nanocomposte fibres was also explored using scanning electron microscopy. In addition, UV absorbance spectra, and tensile and thermal properties of the resulting electrospun mats at different TiO_2 loads were characterized by using UV–vis spectrophotometer, Zwick 1446–60 tensile tester and differential scanning calorimeter respectively.

2 Materials and Methods

Polystyrene (PS) pellets with the weight-average molecular weight (M_w) of 280,000 g/mol and TiO_2 nanoparticles with a particle size of about 25 nm and a specific surface area of about 200-220 m^2/g were received from the Sigma Aldrich. DL-Limonene was purchased from Merck as the solvent. Ethanol was purchased from Merck as the co-solvent. LiCl was one of the commercial products of Pinjiang Chemical Co.

2.1 Preparation of Polymer Solution

A polymer solution with the concentration of 35wt. % was prepared by dissolving PS in a mixture of DL-limonene/methanol (90:10). LiCl (1.5%), as a salt additive, was added into the polymer solution to improve electrical conductivity. The slurry was prepared by dispersing the predetermined amounts of TiO_2 nanoparticles into DL-limonene solvent using ultrasonic vibration for 10 min until the nanoparticles were uniformly dispersed in the solvent. This dispersion of TiO_2 was added into the PS solution and vigorously stirred at ambient temperature for 12h. The compositions of TiO_2 to PS were 0, 2, 4, 6, and 8 wt % and these PS/TiO_2 nanocomposites were referred to as PS-0, PS-2, PS-4, PS-6, and PS-8 respectively.

2.2 Electrospinning Process

The polymer solution was loaded into a glass syringe with a 23 gauge needle. The syringe was fixed horizontally on a syringe pump (Model: STC-527, Terumo Co), in which the polymer solution feed rate and traverse speed of pump were fixed at 0.3 mL/h and 4 cm/min respectively. A 20 kV voltage was applied between the needle and a metallic collector. The tip-to-collector distance of 18 cm was used. Electrospun fibre mats were collected on the rotating drums with the diameter of 15 cm and the rotation speed of 70 rpm. Electrospinning was performed at room temperature for 3h.

2.3 Characterization

Scanning electron microscopy (SEM) of Seron Technology AIS-2100 and field emission scanning electron microscope (FESEM) of Hitachi S-4160 were used to characterize the morphology of

electrospun fibres. At least 100 fibres were used to calculate the mean values of the diameter of electrospun fibres. The fibre diameter distribution was evaluated by a program created in MATLAB 7.

A wide angle X-ray diffraction (WAXD) analysis was performed on samples using a Philips Xpert-MPD X-Ray diffractometer with CuKα radiation (λ=1.54 Å). Scans were run in the wide angle of 5–80 ° and scan speed of 1°/min to confirm the presence of TiO_2 nanoparticles in the fibres and study the crystal form of nanoparticles and fibres in the presence of TiO_2. The fourier transform infrared (FTIR) spectra were obtained on a Gasco 680 plus FTIR spectrometer in the range of 400 - 4000 cm^{-1} by KBr disk method.

The UV absorbance spectra of PS and PS/TiO_2 electrospun mats were recorded by UV–vis spectro photometer (Gasco V-750) in the wavelength range 200 - 800 nm. The sample dimensions were 1× 4 cm (width and length). The thickness of the samples was varied from 120 μm to 140 μm.

The mechanical properties were measured by Zwick 1446–60 tensile tester at the standard conditions. Sample dimensions were 5 mm in width and 15 mm in length with the cross head speed of 5 mm/min. The samples were placed under standard atmospheric conditions (20 ±2˚C and 65±2 % RH) for 24 h before the experiments. Differential scanning calorimeter (DSC) was carried out using TA instrument under a nitrogen atmosphere and a heating rate of 10 °C/min to measure glass transition temperatures (T_g).

3 Results and Discussion

3.1 Morphology of Fibres

The SEM images and diameter distribution diagrams of electrospun PS fibres and PS/TiO_2 nanocomposite fibres are shown in Fig.1. The average diameters of PS and PS/TiO_2 electrospun fibres are listed in Table 1. It is observed that the morphology and diameter of PS electrospun fibres are significantly affected by TiO_2 content. The average of PS/TiO_2 fibres diameter is varied from 1.73 μm to 2.09 μm. SEM micrographs of PS and PS/TiO_2 fibres show that PS microfibres are uniform without any beads. Results also show that the average diameter of PS/TiO_2 nanocomposite fibres is decreased by increasing TiO_2 nanoparticles. The TiO_2 nanoparticles are semiconductor[33] and the addition of TiO_2 nanoparticles increases the electrical conductivity of

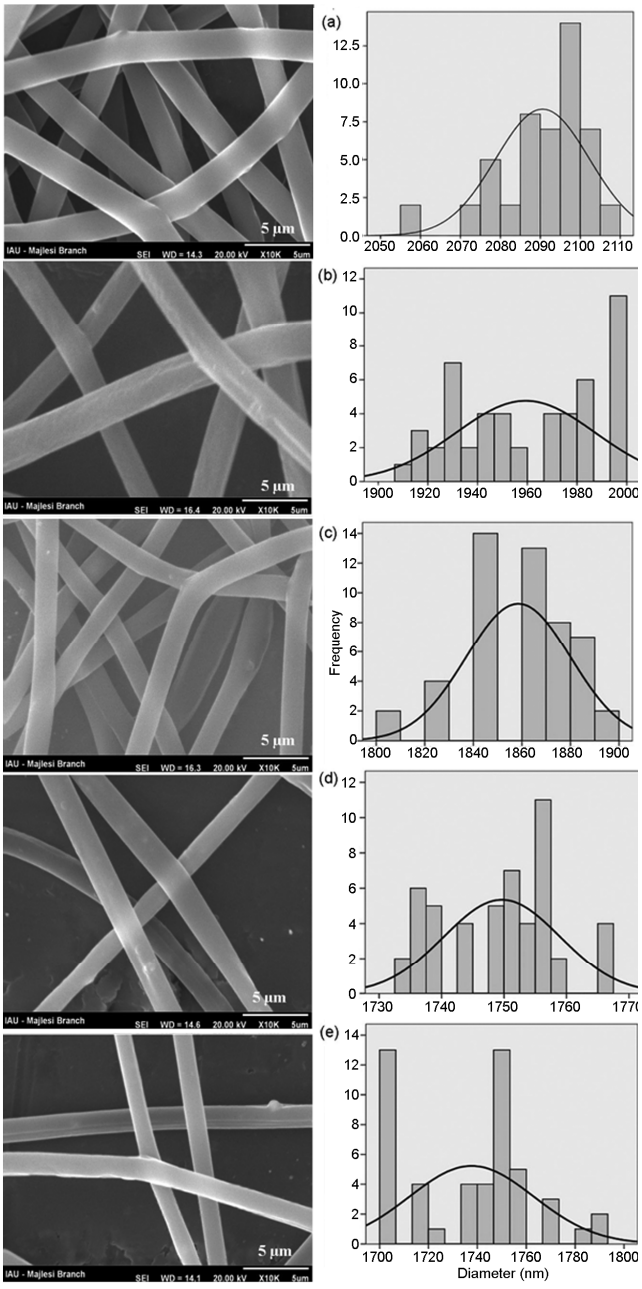

Fig.1—SEM images and nanofibres diameter distribution curves of PS/TiO_2 NC fibres at different TiO_2 contents (a) pure PS, (b) 2% TiO_2; (c) 4% TiO_2; (d) 6% TiO_2, and (e) 8% TiO_2

Table 1—Effect of TiO_2 content on PS electrospun NC fibres diameter and T_g

Sample	TiO_2 content wt %	Diameter μm	T_g °C
PS-0	0	2.09 (1.50)	87
PS-2	2	1.95 (1.42)	-
PS-4	4	1.85 (2.76)	80
PS-6	6	1.74 (3.43)	-
PS-8	8	1.73 (2.56)	79

Values in parentheses show the coefficient of variation.

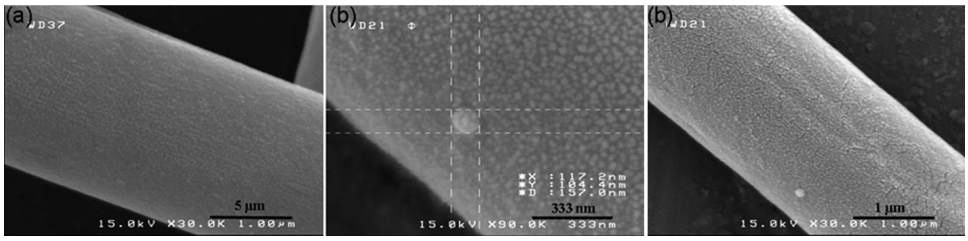

Fig.2—FE-SEM images of (a) pure PS; and (b) PS/TiO_2 NC fibres including 8% wt TiO_2NPs

Table 2—Duncan's multiple- rang test for data of Table 1

Sample	N	Subset for alpha = 0.05			
PS-8	50	1.73	-	-	-
PS-6	50	1.74	-	-	-
PS-4	50	-	1.85	-	-
PS-2	50	-	-	1.95	-
PS-0	50	-	-	-	2.09
Sig.	-	0.486	1.000	1.000	1.000

polymer solution and cause the reduction of PS electrospun fibres diameter. The statistical analysis (Table 2) shows that when TiO_2 nanoparticles content is increased from 0 to 6%, decrease in nanofibres diameter is significant, but when 8% TiO_2 nanoparticles is loaded, decrease in nanofibres diameter is not significant in comparison to nanofibres containing 6% TiO_2 nanoparticles .

The FE-SEM has been used to evaluate the dispersion of TiO_2 nanoparticles on the surface of PS nanocomposite fibres. The FE-SEM images of pure PS fibres and PS/TiO_2 nanocomposite fibres containing 8%wt TiO_2 nanoparticles can be observed in Fig. 2. These images show some agglomeration of TiO_2 nanoparticles on the surface of electrospun fibres (Fig. 2b). It can be observed from Fig. 2(b) that the size of some TiO_2 nanoparticles is about 117 nm. The aggregation of TiO_2 nanoparticles is due to the hydrophobic nature of PS and there is not enough steric hindrance[34].

3.2 X-ray Diffraction Analysis

The wide angle X-ray diffraction patterns of TiO_2 nanoparticles, PS electrospun fibres and PS/TiO_2 nanocomposite fibres containing 8 wt% nanoparticles are shown in Fig. 3. TiO_2 nanoparticles show two diffraction peaks at 2θ=25° and 48°, which belong to (101) and (200) plane reflection of TiO_2 respectively, thereby indicating that TiO_2 is in the anatase phase[35]. A broad diffraction peak at about 2θ=20° is observed in PS fibres corresponding to the PS noncrystalline phase. As indicated in Fig. 3c, apart from the diffraction peak of PS, only one of the diffraction peaks at about 2θ=26° can be indexed as the anatase

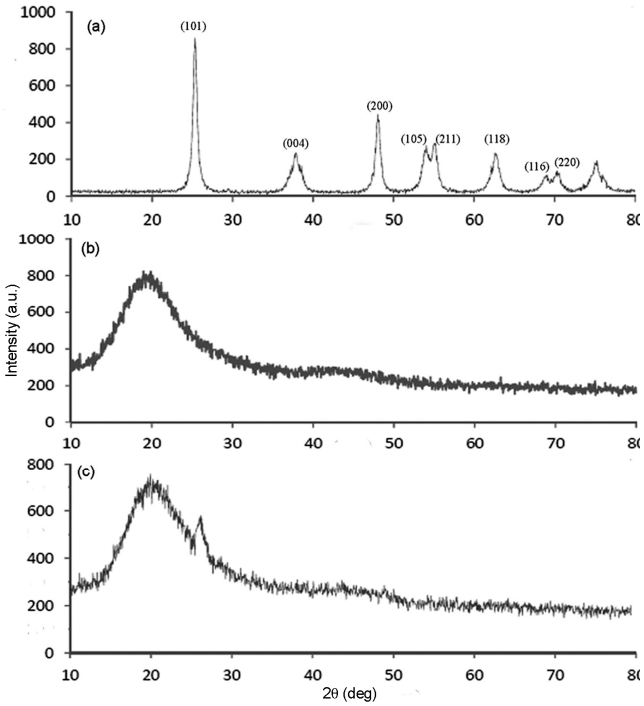

Fig.3—X-ray diffraction spectra of (a) TiO_2 NPs, (b) electrospun PS fibres, and (c) electrospun PS fibres containing 8 wt% TiO_2 NPs

phase of TiO_2 for PS/TiO_2 nanocomposite fibres loaded with 8 wt. % TiO_2. This observation can be attributed to the small amount of TiO_2 in the PS fibres.

3.3 FTIR Spectroscopy

In order to evaluate the chemical interaction between the PS and the TiO_2 nanoparticles, FTIR measurements are performed. Figure 4 shows FTIR spectra of TiO_2, PS electrospun fibres and PS/TiO_2 nanocomposite fibres. The characteristic peak of TiO_2 nanoparticles is a strong kind of absorption peak that appears at about 533 cm^{-1}. FTIR spectrum of PS (Fig. 4b) shows several characteristic peaks, such as the aromatic C=C stretching vibration peaks at 1400-1600 cm^{-1} , 700 and 750 cm^{-1} (monosubstituted benzene). The absorption bands at 3083, 3061 and 3026 cm^{-1} are all associated with unsaturated C-H stretching vibration in the phenyl ring of PS. The bands assigned to C-H bending vibration appear at

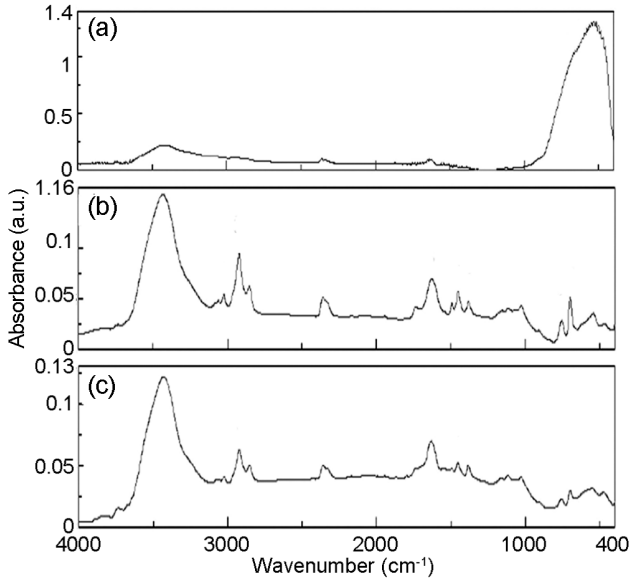

Fig.4—FTIR spectra of (a) TiO_2 NPs, (b) PS, and (c) PS/TiO_2 NC fibres with 8 wt% TiO_2

1452 and 1493 cm^{-1}. The peaks at 755 and 698 cm^{-1} show the C–H stretches in the monosubstituent of the aromatic ring. No significant differences between the FTIR spectra for both materials are noticed. Pure PS and PS/ TiO_2 nanocomposite fibres present the same FTIR spectra. The addition of TiO_2 nanoparticles does not shift or change absorption band in electrospun nanocomposite fibres. This indicates that there is no chemical interaction between PS and TiO_2 nanoparticles in the resulting composite fibres. Also, since the amount of nanoparticles in the sample is negligible with respect to polymer, no peak from nanoparticles in nanocomposite spectrum is observed.

3.4 Thermal Analysis of Fibres

Figure 5 shows the DSC thermographs of electrospun PS and PS/TiO_2 nanocomposite fibres. Table 1 compares the results of glass transition temperatures (T_g) of these samples as determined from the DSC thermographs. These results show that T_g of PS fibres is decreased as the concentration of TiO_2 in PS is increased. The T_g value could be attributed to the polymer chains mobility. So, the decrease in T_g value of PS/TiO_2 fibres by the increase in TiO_2 nanoparticles content is due to the enhancement of the mobility of polymer chains. In other words, TiO_2 nanoparticles act as plasticizers. In fact, plasticizers work by embedding themselves between the chains of polymers, spacing them apart (increasing the free volume), and as a result, lowering the glass transition temperature for the plastic, thus making it softer. So,

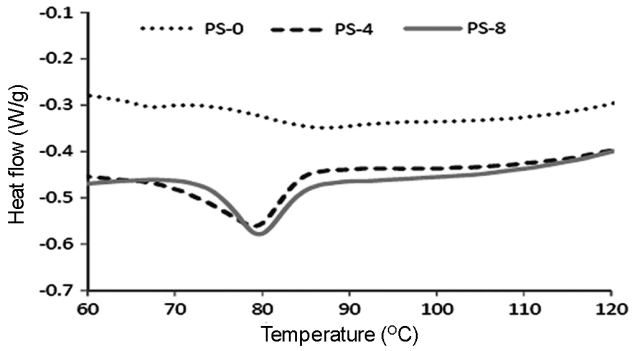

Fig.5—DSC curves of PS/TiO_2 electrospun fibres with different NPs contents

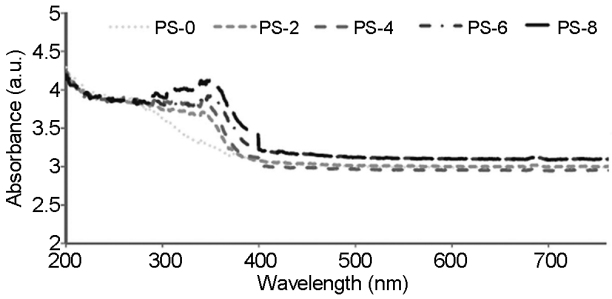

Fig.6—Absorbance spectra in the UV–vis of pure PS and PS/TiO2 electrospun fibres

it can be said that these nanoparticles decrease T_g of PS/TiO_2 electrospun fibres by increasing the free volume of polymer. The same results are reported by Kim *et al*[31] for PS/Au nanocomposite fibres.

3.5 UV-vis Spectra of Electrospun PS/TiO_2 Nanocomposite Fibres

Figure 6 shows the absorbance spectra of PS and PS/TiO_2 electrospun fibres in the ultraviolet and visible region (190- 700 nm) of electromagnetic spectrum. The addition of TiO_2 nanoparticles increases the absorbance values at all wavelengths of UV region. Based on the results, the maximum absorption by samples is located at about 340 nm, which is shifted to higher wavelengths by the increase in TiO_2 content. For this point, the absorption is decreased by wavelength increase at 400 nm. As a result of loaded TiO_2 nanoparticles, the UV protection of PS electrospun fibres is increased. UV protection of PS/TiO_2 nanocomposite fibres is due to the scattering of UV rays through the high refractive index of TiO_2 and/or absorption of UV rays because of the semiconductive properties of TiO_2 [36].

3.6 Mechanical Properties of Electrospun PS/TiO_2 Nanocomposite Fibres

Several parameters such as particle-matrix interface adhesion, particle size, particle dispersion

Table 3—Mechanical properties of PS and PS/TiO_2 electrospun mats

Sample	Tensile strength MPa	Modulus MPa	Elongation at break %
PS-0	1.37 ± 0.73	41.77 ± 28.7	1.69 ± 0.57
PS-2	1.9 ± 0.51	67.21 ± 21.48	2.85 ± 0.65
PS-4	3.26± 0.49	93.36 ±15.41	2.76 ± 1.08
PS-6	2.48 ± 0.37	64.64 ±18.17	3.87 ± 0.7
PS-8	2.05 ± 0.29	60.73 ± 15.17	3.28 ± 0.78

Table 4—Duncan's multiple- rang test for tensile strength and modulus data of Table 3

Sample	N	Subset for alpha = 0.05				
		Tensile strength				
PS-0	5	1.3700				
PS-2	5		1.9000			
PS-8	5			2.0500		
PS-6	5				2.4800	
PS-4	5					3.2600
Sig.		1.000	1.000	1.000	1.000	1.000
		Modulus				
PS-0	5	41.7700				
PS-8	5		60.7300			
PS-6	5			64.6400		
PS-2	5				67.2100	
PS-4	5					93.3600
Sig.		1.000	1.000	1.000	1.000	1.000

and particle loading influence the mechanical properties of composites[37]. The variations in tensile properties of PS and PS/TiO_2 electrospun mats with TiO_2 content are listed in Table 3. As can be seen, the tensile strength and modulus of electrospun mats are increased with the increase in nanoparticles content up to 4 wt% above, showing a tendency to decrease with the increase of nanoparticles loading. With the high amount of nanoparticles above 4 wt%, the tensile strength and modulus decrease. This could be due to the aggregation of nanoparticles. As shown in Table 4, the increase in TiO_2 nanoparticles content makes significant difference in the strength and modulus of nanofibre mats. Tensile strength of nanocomposites can be enhanced when interfacial adhesion is improved. This can be correlated to the interaction of filler with the matrix. Therefore, well-adhering nano-TiO_2 can bear on the part of the load applied to the matrix and contributes to the tensile strength of the nanocomposites[38].

4 Conclusion

SEM images show that the PS fibre diameter decreases by increasing TiO_2 nanoparticles content. FE-SEM images reveal the aggregation of TiO_2 nanoparticles in the PS nanocomposite fibres with 8%wt nanoparticles. Results obtained from X-ray diffraction of electrospun fibres bearing nanoparticles confirm the presence of nanoparticles in the samples. Investigating the FTIR spectrum of nanoparticles, pure PS and PS/TiO_2 nanocomposite fibres also show no change in the position of PS peaks or creation of a new peak in nanocomposite spectrum. This analysis indicates that there is only physical mixing of polymer and nanoparticles. Evaluating the effect of the amount TiO_2 nanoparticles on the mechanical properties of electrospun webs show that the increase in tensile strength and modulus with the increase of nanoparticles value is followed by a decrease beyond 4 wt%. Furthermore, considering the differential scanning calorimeter of PS electrospun fibres it is proved that by increasing the amount of TiO_2 nanoparticles, the glass transition temperature could be decreased.

References

1 Huang Z M, Zhang Y Z, Kotaki M & Ramakrishna S, *Compos Sci Technol ,* 63 (2003) 2223.
2 Subbiah T, Bhat G S, Tock R W, Parameswaran S & Ramkumar S S, *J Appl Polym Sci,* 96 (2005) 557.
3 Andrady A L, *Science and Technology of Polymer Nanofibers* (Wiley Publishing Limited, USA) 2008.
4 Ramakrishna S, Fujihara K, Teo W E, Lim T C & Ma Z, *An Introduction in Electrospinning and Nanofibers* (World Scientific Publishing Co Pte Ltdm Singapore) 2005.
5 Brown P J & Stevens K, *Nanofibers and Nanotechnology in the Textiles* (Woodhead Publishing Limited, England) 2007.
6 Mallakpour S & Rafiee Z, *Polystyrene* (Iranian Polymer Society) 2010.
7 Shin C, An H & Chase G G, *Chem Eng Technol,* 29 (2006) 364.
8 An H, Shin C & Chase G G, *J Membrane Sci,* 283 (2006) 84.
9 Shin C, *J Colloid Interf Sci,* 302 (2006) 267.
10 Baker S C, Atkin N, Gunning P A, Granville N, Wilson K, Wilson D & Southgate J, *Biomaterials,* 27 (2006) 3136.
11 Feng Sh & Shen X, *J Macromol Sci B,* 49 (2010) 345.
12 Zheng J, He A, Li J, Xu J & Han C C, *Polymer,* 47 (2006) 7095.
13 Lin T, Wang Ho, Wang Hu & Wang X, *Nanotechnology,* 15 (2004) 1375.
14 Kim G T, Hwang Y J, Ahn Y Ch, Shin H S, Lee J K & Sung Ch M, *Korean J Chem Eng ,* 22 (2005) 147.
15 Casper Ch L, Stephens J S, Tassi N G, Chase D B & Rabolt J F, *Macromolecules,* 37 (2004) 573.
16 Eda G & Shivkumar S, *J Mater Sci,* 41 (2006) 5704.
17 Lee K H, Kim H Y, Bang H J, Jung Y H & Lee S G, *Polymer,* 44 (2003) 4029.
18 Demir M M, *EXPRESS Polym Lett,* 4 (2010) 2.

19 Pattamaprom C, Hongrojjanawiwat W, Koombhongse P, Supaphol P, Jarusuwannapoo T & Rangkupan R, *Macromol Mater Eng,* 291 (2006) 840.

20 Jarusuwannapoom T, Hongrojjanawiwat W, Jitjaicham S, Wannatong L, Nithitanakul M, Pattamaprom C, Koombhongse P, Rangkupan R & Supaphol P, *Eur Polym J,* 41 (2005) 409.

21 Eda G, Liu J & Shivkumar S, *Eur Polym J,* 43 (2007) 1154.

22 Uyar T & Besenbacher F, *Polymer,* 49 (2008) 5336.

23 Wannatong L, Sirivat A & Supaphol P, *Polym Int,* 53 (2004) 1851.

24 García M T, Duque G, Gracia I, Lucas A D & Rodríguez J F, *J Mater Cycles Waste Manage ,* 11 (2009) 2.

25 Noguchi T, Miyashita M, Inagaki Y & Watanabe H, *Packag Technol Sci,* 11 (1998) 19.

26 Shin Ch & Chase G G, *Polym Bull,* 55 (2005) 209.

27 Atti-Santos A C, Rossato M, Serafini L A, Cassel E & Moyna P, *Braz Arch Biol Techn,* 48 (2005) 155.

28 Mazinani S, Ajji A & Dubois Ch, *Polymer,* 50 (2008) 3329.

29 Chen X, Wei S, Gunesoglu C, Zhu J, Southworth C S, Sun L, Karki A B, Young D P & Guo Z, *Macromol Chem Phys,* 211 (2010) 1775.

30 Rojas O J, Montero G A & Habibi Y, *J Appl Polym Sci,* 113 (2009) 927.

31 Kim J K & Ahn H, *Macromol Res,* 6 (2008) 163.

32 Kobayashi M, Egashira M & Konno T, *Mater Sci Forum,* 561-565 (2007) 663.

33 Jeong B-S Norton D P & Budai J D, *Solid State Electron*, 47 (2003) 2275.

34 Zan L, Tian L, Liu Z & Peng Z, *Appl Catal A-Gen,* 264 (2004) 237.

35 Thamaphat Kh, Limsuwan P & Ngotawornchai B, *Kasetsart J (Nat Sci),* 42 (2008) 357.

36 Erdem N, Erdogan U H, Cireli A A & Onar N, *J Appl Polym Sci,* 115 (2010) 152.

37 Fu Sh Y, Feng X Q, Lauke B & Mai Y W, *Compos Part B-Eng* 39 (2008) 933.

38 Selvin T P, Kuruvilla J & Sabu T, *Mater Lett* 58 (2004) 281.